Comparative Study on Sensorless Vibration Suppression of Fast Moving Flexible Linear Robots

F. Johannes Kilian, Hubert Gattringer, Klemens Springer, and Hartmut Bremer

Institute for Robotics, Johannes Kepler University Linz, Altenbergerstr. 69, 4040 Linz, Austria
{johannes.kilian,hubert.gattringer,klemens.springer, hartmut.bremer}@jku.at
http://www.robotik.jku.at

Abstract. This contribution introduces three sensorless vibration suppression methods for flexible, fast moving linear robots. After some investigations concerning the required mathematical models of the flexible linear robot, several vibration suppression techniques are derived in detail. The main idea of all concepts is the specific modification of an arbitrary trajectory in real time. Therefore, all conventional control concepts of the robot may remain unchanged. The application of each technique leads nearly to a complete annihilation of the TCP vibrations immediately after the end of the trajectory. For this reason, the implementation of these methods allows much higher velocities and therefore lower cycle times in nearly every manipulation process. Over and above, these vibration suppression methods enable light-weight construction and therefore lower energy consumption and represent an important step to increase velocity and energy efficiency in automation processes.

Keywords: Linear Robots, Sensorless Vibration Suppression, Elastic Multibody System, Flatness-based Control, Ritz Approximation.

1 Introduction

In the last few years the automation industry has taken great steps in order to increase velocity and accuracy of robots as well as to reduce cycle times and energy consumption. For this reason the reduction of mass and inertia seems to be the best possibility to manage both requirements. Unfortunately, the reduction of mass and inertia in combination with higher velocities leads to undesirable structural vibrations, which must be avoided or suppressed to achieve a high position accuracy.

Common vibration suppression methods use measurements of the tool center point (TCP) to damp the vibrations of a flexible linear robot, see e.g. [1], [2], [3], [4] and [5]. Instead of reacting on the TCP vibrations, the presented methods act at a previous step and try to avoid the vibrations caused by a movement

R. Moreno-Díaz et al. (Eds.): EUROCAST 2013, Part II, LNCS 8112, pp. 305–312, 2013.

completely. Therefore, the desired and arbitrary trajectory is modified in real time in such a way that the resulting trajectory will not induce oscillations. All presented methods do not require additional sensors if the vibrations are caused by the robot's own movement.

The considered paper is organized as follows. After a detailed description of the linear robot in section 2, section 3 gives an overview of the used dynamical models. Section 4 deals with the derivation of three vibration suppression methods. Experimental results conclude the contribution in section 5.

2 Flexible Linear Robot

The considered linear robot is shown in Fig. 1. Three linear axes are connected by flexible beams and driven by synchronous motors via elastic gear racks. The positions of the axes are measured via resolvers connected to the motors. According to the robot design variants, the third axis consists of either one or two kinematically coupled flexible beams. The entire robot is mounted on a pedestal, whose structural elasticities are modeled by rotating springs in two directions ($\varphi_1(t)$ and $\varphi_2(t)$). The main elastic influences of the axes 1 and 2 are bending in two directions ($v(x,t)$ and $w(x,t)$) and torsion in one direction ($\vartheta(x,t)$). Due to the layout of the elastic beams of the third axis, torsion can be neglected whereby only bending in two directions is taken into account. All in all, we consider this linear robot with 12 elastic degrees of freedom, 7 degrees of freedom to describe bearing and gear deflections and 3 translational degrees of freedom. For control design, the detailed model of Fig. 1 (a) must be simplified. Therefore, we approximate the structure elasticities and bearings with rigid bodies and linear spring-damper systems and obtain a less complex model of the flexible linear robot, see Fig. 1 (b). This lumped element model (LEM) serves as basis for several methods of vibration suppression.

3 Dynamical Model

To achieve the equations of motion the Projection Equation (see [6] for details) in subsystem representation

$$\sum_{n=1}^{N_{sub}} \left(\left(\frac{\partial \dot{\mathbf{y}}_n}{\partial \dot{\mathbf{q}}} \right)^T \sum_{i=1}^{N_n} \left[\left(\frac{\partial \mathbf{v}_c}{\partial \dot{\mathbf{y}}_n} \right)^T \left(\frac{\partial \boldsymbol{\omega}_c}{\partial \dot{\mathbf{y}}_n} \right)^T \right]_i \begin{pmatrix} \dot{\mathbf{p}} + \widetilde{\boldsymbol{\omega}}_0 \mathbf{p} - \mathbf{f}^e \\ \dot{\mathbf{L}} + \widetilde{\boldsymbol{\omega}}_0 \mathbf{L} - \mathbf{M}^e \end{pmatrix}_i + \int_{B_n} \left(\frac{\partial \dot{\mathbf{y}}_n}{\partial \dot{\mathbf{q}}} \right)^T \left[\left(\frac{\partial \mathbf{v}_c}{\partial \dot{\mathbf{y}}_n} \right)^T \left(\frac{\partial \boldsymbol{\omega}_c}{\partial \dot{\mathbf{y}}_n} \right)^T \right] \begin{pmatrix} d\dot{\mathbf{p}} + \widetilde{\boldsymbol{\omega}}_0 d\mathbf{p} - d\mathbf{f}^e \\ d\dot{\mathbf{L}} + \widetilde{\boldsymbol{\omega}}_0 d\mathbf{L} - d\mathbf{M}^e \end{pmatrix} \right) = 0, \tag{1}$$

is used. This synthetical method emerges as good possibility to calculate the equations of motion for linear, articulated, rigid or elastic robots. According to the linear robot with structural elasticities, a Ritz approximation separates the

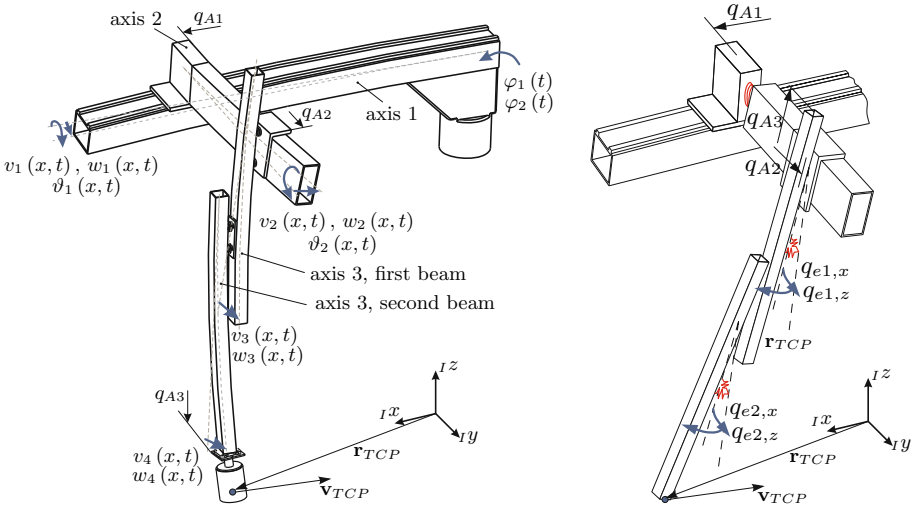

(a) Schematic view of the fexible, linear robot with the structural elasticities

(b) Lumped element model of the linear, elastic robot

Fig. 1. Schematic view of the linear robot with structural elasticities (a) and of the lumped element model (LEM) (b) including the degrees of freedom

distributed parameters into shape functions and Ritz coefficients and therefore yields nonlinear, ordinary differential equations of motion

$$\mathbf{M}(\mathbf{q})\,\ddot{\mathbf{q}} + \mathbf{g}(\mathbf{q}, \dot{\mathbf{q}}) - \mathbf{Q} = 0, \tag{2}$$

see [7] for a detailed derivation of the equations of motion for this specific robot. The dynamical model of the LEM is derived in an equivalent manner and yields less complicated equations of motion. For more information considering the modeling method we refer to [6], [7], [8] and [9].

In order to simplify the LEM for a flat parametrization, the equations of motion are axis-decoupled and linearized regarding the elastic angles q_e. Neglecting damping effects, we thereby obtain

$$\begin{bmatrix} M_{MM} & \mathbf{M}_{Me} \\ \mathbf{M}_{eM} & \mathbf{M}_{ee} \end{bmatrix} \begin{pmatrix} \ddot{q}_A \\ \ddot{\mathbf{q}}_e \end{pmatrix} + \begin{bmatrix} 0 & 0 \\ 0 & \mathbf{c}_e \end{bmatrix} \begin{pmatrix} q_A \\ \mathbf{q}_e \end{pmatrix} = \begin{pmatrix} \mathbf{Q} \\ 0 \end{pmatrix} \tag{3}$$

for axis 1 and axis 2. After some sophisticated investigations, we receive a flat output for each axis i

$$y_i = q_{A,i} + k_{1,i}\, q_{ei,1} + k_{2,i}\, q_{ei,2}, \tag{4}$$

using the elastic angles q_{ei} and the parameters $k_{1,i}$ and $k_{2,i}$. This flat parametrization enables the calculation of the system states as algebraic functions of the flat output and its time derivatives

$$q_{A,i} = \Psi_1 \left(y_i, \dot{y}_i, \ddot{y}_i, \ldots \right) \tag{5}$$

$$q_{ei,1} = \Psi_2 \left(y_i, \dot{y}_i, \ddot{y}_i, \ldots \right) \tag{6}$$

$$q_{ei,2} = \Psi_3 \left(y_i, \dot{y}_i, \ddot{y}_i, \ldots \right). \tag{7}$$

A comparison between this flat output and the position of the tool-center-point (TCP) $\mathbf{r}_{TCP}$ shows a high accordance. This fact is the basis for the flatness-based correction of the motor angles, which is described in the following section in detail.

4 Vibration Suppression Methods

Beside the great number of vibration suppression methods, only three of them are outlined and compared in this paper. The collective principle of all presented methods is the modification $\mathbf{q}_{M,d,mod}$ of the desired trajectory $\mathbf{q}_{M,d}$ in a very tiny manner in order to reduce the elastic deflections, which arise from the movement itself. Additionally, the conventional, decentralized position controller of the robot serves as basis for all concepts and is not modified for the vibration suppression. This leads to a simple implementation because the conventional control architecture remains unchanged, see Fig. 2.

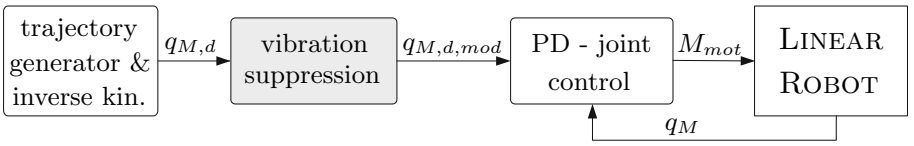

Fig. 2. Scheme of the control architecture including the sensorless vibration suppression

The following three vibration suppression techniques are described in detail:

(a) compensation of the elastic deflection via a Taylor expansion
(b) flatness-based correction of the motor angles
(c) generation of preshaping command inputs (input shaping).

4.1 Compensation of the Elastic Deflection

The compensation of the elastic deflections is based on the equations of motion of the flexible, linear robot with structural elasticities using the minimal coordinates $\mathbf{q}^T = \left(\mathbf{q}_M^T \, \mathbf{q}_A^T \, \mathbf{q}_e^T \right)$ - with the motor coordinates $\mathbf{q}_M$, the arm coordinates $\mathbf{q}_A$ and the Ritz coefficients $\mathbf{q}_e$. A Taylor expansion of (2) $\mathbf{q}^T = \mathbf{q}_0^T + \mathbf{y}^T = \left(\mathbf{q}_{ref}^T \, \mathbf{q}_{ref}^T \, 0 \right) + \left(\mathbf{y}_M^T \, \mathbf{y}_A^T \, \mathbf{q}_e^T \right)$ along a reference path $\mathbf{q}_0$ yields

$$\underbrace{\begin{bmatrix} \mathbf{M}_{MM} & \mathbf{M}_{MA} & \mathbf{M}_{Me} \\ \mathbf{M}_{MA}^T & \mathbf{M}_{AA} & \mathbf{M}_{Ae} \\ \mathbf{M}_{Me}^T & \mathbf{M}_{Ae}^T & \mathbf{M}_{ee} \end{bmatrix} \begin{bmatrix} \ddot{\mathbf{q}}_{ref} \\ \ddot{\mathbf{q}}_{ref} \\ \mathbf{0} \end{bmatrix} + \begin{bmatrix} \mathbf{g}_{0,M} \\ \mathbf{g}_{0,A} \\ \mathbf{g}_{0,e} \end{bmatrix} - \begin{bmatrix} \mathbf{u}_0 \\ \mathbf{0} \\ \mathbf{0} \end{bmatrix}}_{-\mathbf{h}_0} +$$

$$\mathbf{M}(\mathbf{q}_0)\,\ddot{\mathbf{y}} + \mathbf{P}_0\,\dot{\mathbf{y}} + \mathbf{Q}_0\,\mathbf{y} = \begin{pmatrix} \mathbf{u}_c \\ \mathbf{0} \\ \mathbf{0} \end{pmatrix}.$$

The feed-forward input $\mathbf{u}_0$ can be calculated using the first two rows of the error vector $\mathbf{h}_0$ for a rigid body system. The input $\mathbf{u}_c$ stands for the resulting torque of the PD - joint control. Neglecting the influence of $\mathbf{M}_0$ and $\mathbf{P}_0$ leads to a quasi-static approximation and enables the algebraic calculation of the elastic deflections $\mathbf{y}_Q = \left(\mathbf{y}_{MQ}^T\,\mathbf{y}_{AQ}^T\,\mathbf{q}_{eQ}^T\right)^T = \mathbf{Q}_0^{-1}\,\mathbf{h}_0$. Therefore, the deflections $\mathbf{y}_Q$ only depend on the reference trajectory $\mathbf{q}_{ref}$ and should be compensated by correction $\Delta\,\mathbf{q}_{ref}$ of the reference path. Both influences on the TCP position can be calculated by the Jacbobians

$$\Delta\,\mathbf{r}_{TCP} = \underbrace{\begin{bmatrix} \dfrac{\partial\,\mathbf{v}_{TCP}}{\partial\dot{\mathbf{q}}_A} & \dfrac{\partial\,\mathbf{v}_{TCP}}{\partial\dot{\mathbf{q}}_e} \end{bmatrix}}_{\mathbf{F}_{TCP}} \begin{pmatrix} \mathbf{y}_A \\ \mathbf{q}_e \end{pmatrix}, \quad \Delta\,\mathbf{r}_{TCP,ref} = \underbrace{\begin{bmatrix} \dfrac{\partial\,\mathbf{v}_{TCP}}{\partial\dot{\mathbf{q}}_{ref}} \end{bmatrix}}_{\mathbf{F}_{TCP,ref}} \Delta\mathbf{q}_{ref}. \quad (8)$$

The compensation of the elastic deflections requires $\Delta\mathbf{r}_{TCP} + \Delta\mathbf{r}_{TCP,ref} = 0$ and delivers the input error correction of the reference path

$$\Delta\,\mathbf{q}_{ref} = \mathbf{F}_{TCP,ref}^{+}\,\mathbf{F}_{TCP} \begin{pmatrix} \mathbf{y}_A \\ \mathbf{q}_e \end{pmatrix}. \quad (9)$$

This leads to a new desired motor position $\mathbf{q}_{M,d,mod} = \mathbf{q}_{ref} + \Delta\mathbf{q}_{ref}$. For detailed information according this vibration suppression method we refer to [6], [9], [10] and [11].

4.2 Flatness-Based Correction of the Motor Angles

The LEM shown in (3) - neglecting bearing and gear deflections ($\mathbf{q}_M = \mathbf{q}_A$) - provides the basis for the flatness-based correction of the motor angles. The subsequent flat parametrization delivers the ability to compute the motor angles $\mathbf{q}_M$ as function of the flat output, see (5). Due to the high accordance between the flat output and the TCP position $\mathbf{r}_{TCP}$, (5) gives the possibility to calculate a new desired motor position $\mathbf{q}_{M,d,mod}$ as function of the TCP position. This modified motor angle serves as input for the conventional, decentralized PD - joint control (see Fig. 2) and leads to a movement that does not induce vibrations.

4.3 Input Shaping

Input shaping techniques originally arise from the subject of crane trajectory generation and base on the ideas of N. Singer and W. Seering (see [12] for details).

The input shaper rearranges the desired trajectory using a convolution with a progression of Dirac delta functions, see Fig. 3. The result of this mathematical operation yields a trajectory which does not induce vibrations and reaches the final position including a small, but constant time delay.

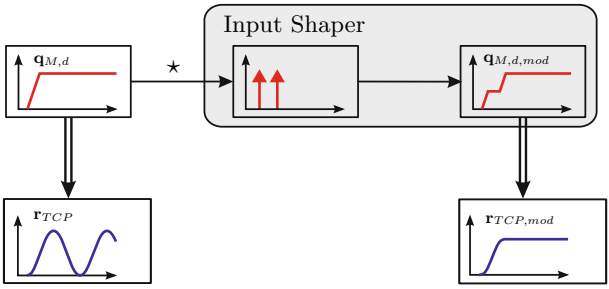

Fig. 3. Procedure of the input shaper vibration suppression method

The literature gives us several input shaping methods in order to design the number, amplitude and point of actuation of the Dirac delta functions. These design parameters lead to differences in the percentage of remaining vibrations, in the sensitivity according to model inaccuracies and in the time delay, which increases with each additional Dirac delta function. For every input shaper design, the eigenfrequency and the system damping of the linear robot considering the TCP vibrations, has to be well-known. These two parameters arise from the eigenvalues of the linearized LEM of the linear robot. Four different types of input shaper

- Zero Vibration (ZV)
- Zero Vibration and Derivative (ZVD)
- Extra Insensitive (EI)
- Zero Vibration and Double Derivative (ZVDD)

are designed and compared in the following section. A detailed derivation of each design method can be found in [12]. Figure 4 shows the time delay and the sensitivity of several input shapers by comparing their measured percentage of remaining TCP vibrations for various tip mass errors $\Delta m = m_{tipmass,design} - m_{tipmass,real}$. Obviously, those input shapers, which use a higher number of Dirac delta functions, enable a higher robustness, but also own higher time delays.

5 Experimental Results

In order to conclude the comparative study, all presented sensorless vibration suppression methods are implemented on the real robot. The measurement of TCP accelerations in Fig. 5 during an accelerating and decelerating phase of

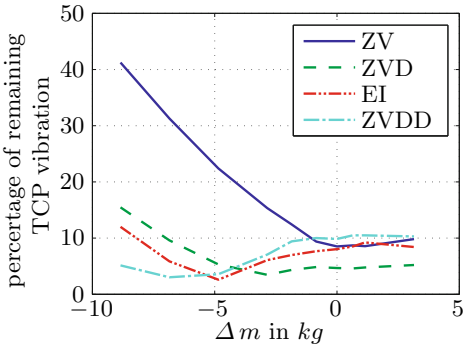

Input Shaper	time delay in ms
ZV	60
ZVD	120
EI	120
ZVDD	180

Fig. 4. Measurement results considering the insensitivity and time delay of various input shaper designs

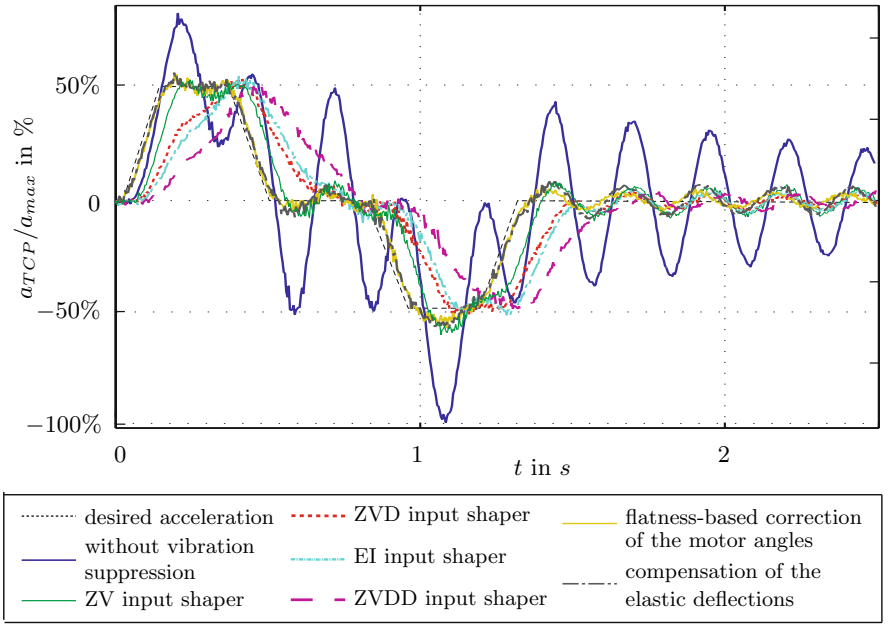

Fig. 5. TCP acceleration for several vibration suppression methods during a trajectory in direction of q_{A1}

a trajectory in q_{A1}-direction enables a clear comparison. Trajectories in q_{A2}-direction deliver equivalent results and may be skipped at this point. It seems evident that nearly all vibration suppression methods show equal measurement results. Whereas the flatness-based correction of the motor angles and the compensation of the elastic deflections provide almost identical performance, the input shaping methods differ in their time delays. Although a very small amplitude of vibrations remains at the TCP, no accelerations are visible after the end of the trajectory.

This comparative study shows the high performance and the industrial usability of the presented methods. All of them reduce the TCP vibrations to a negligible amplitude by a small correction of the desired trajectory using the conventional control architecture.

Acknowledgment. The authors gratefully acknowledge support of the *Austrian Research Promotion Agency* (FFG) and the *Austrian Center of Competence in Mechatronics* (ACCM) for the present work.

References

1. Staufer, P., Gattringer, H., Höbarth, W., Bremer, H.: Passivity Based Backstepping Control of an Elastic Robot. In: ROMANSY 18 Robot Design, Dynamics and Control, vol. 524, pp. 315–322 (2010)
2. Staufer, P., Gattringer, H., Bremer, H.: Vibration Suppression for a Flexible Link Robot using Acceleration and/or Angular Rate Measurements and a Flatness Based Trajectory Control. In: Proceedings of the ASME IDETC/CIE 2011, Washington (2011)
3. Staufer, P., Gattringer, H.: State Estimation on Flexible Robots using Accelerometers and Angular Rate Sensors. In: Mechatronics 2012, pp. 1043–1049 (2012)
4. Bernzen, W.: Active Vibration Control of Flexible Robots using Virtual Spring-Damper Systems. Journal of Intelligent Robotics Systems 24, 69–88 (1999)
5. Dumetz, E., Dieulot, J.-Y., Barre, P.-J., Colas, F., Delplace, T.: Control of an Industrial Robot using Acceleration Feedback. Journal for Intelligent Robots and Systems 46 (2006)
6. Bremer, H.: Elastic Multibody Dynamics - A Direct Ritz Approach. Springer, Heidelberg (2008)
7. Kilian, F.J., Gattringer, H., Bremer, H.: Dynamical Modeling of Flexible Linear Robots. In: Proceedings of the ASME IDETC/CIE 2011, Washington, pp. 899–908 (2011)
8. Gattringer, H.: Starr-elastische Robotersysteme - Theorie und Anwendung. Springer, Heidelberg (2011)
9. Gattringer, H., Kilian, F.J., Höbarth, W., Bremer, H.: Modeling and Vibration Suppression for Fast Moving Linear Robots. In: Proceedings of International Conference of Numerical Analysis and Applied Mathematics 2010, Rhodos (2010)
10. Höbarth, W., Gattringer, H., Bremer, H.: Control Strategies for a Hybrid Articulated Robot. In: 81st Annual Meeting of the International Association of Applied Mathematics and Mechanics (GAMM), vol. 10(1), pp. 39–40 (2010)
11. Höbarth, W., Gattringer, H., Staufer, P., Bremer, H.: Modelling and Control of an Articulated Robot with Flexible Links/Joints. In: Proceedings of the 9th International Conference on Motion and Vibration Control MOVIC (2008)
12. Singer, N.C., Seering, W.P.: Preshaping Command Inputs to Reduce System Vibration. ASME Journal of Dynamic Systems, Measurement and Control 112, 76–82 (1990)